

# Modeling Air Flow Dynamics in Radon Mitigation Systems: A Simplified Approach

T. A. Reddy, K. J. Gadsby, H. E. Black, III, D. T. Harrie

Center for Energy and Environmental Studies  
Princeton University,  
Princeton, New Jersey

R. G. Sextro

Indoor Environment Program  
Lawrence Berkeley Laboratory  
Berkeley, California

Subslab air flow dynamics provide important diagnostic information for designing optimal radon mitigation systems based on the subslab depressurization technique. In this paper, it is suggested that subslab air flow induced by a central suction point be treated as radial air flow through a porous bed contained between two impermeable disks. Next, we show that subslab air flow is most likely to be turbulent under actual field situations in houses with subslab gravel beds, while remaining laminar when soil is present under the slab. The physical significance of this model is discussed and simplified closed-form equations are derived to predict pressure and flows at various distances from a single central depressurization point. A laboratory apparatus was built in order to verify our model and experimentally determine the model coefficients of the pressure drop versus flow for commonly encountered subslab gravel materials. These pressure drop coefficients can be used in conjunction with our simplified model as a rational means of assessing subslab connectivity in actual houses, which is an important aspect of the pre-mitigation diagnostic phase. Preliminary field verification results in a house with gravel under the basement slab are presented and discussed.

## Implications

The most widely used method for radon mitigation in residences is the subslab depressurization technique. This method involves depressurizing the area underneath the slab, causing venting and removal of soil radon directly into the ambient air. It has been found that, very often, such systems are either underdesigned (i.e., unable to reduce indoor radon concentrations to the desired level), or overdesigned (in which case, there is an increase in the energy consumption for heating and cooling and a risk of elevated ambient radon concentrations). In order to avoid these extremes, there is a need to develop subslab diagnostic protocols to aid in the proper design of subslab depressurization systems. This paper suggests a simple mathematical model for assessing subslab air flow dynamics and describes experimental results performed, both in the laboratory and in the field, which substantiate the model approach.

An EPA sponsored workshop was held at Princeton University in order to summarize available knowledge on various radon diagnostic techniques.<sup>1</sup> The emphasis of the workshop was on diagnostics because every home, housing division, and region has different characteristics affecting radon entry. These, in turn, require that special attention be paid to system design in order to maximize mitigation performance and minimize cost. This is especially important since it appears that a large number of houses which have been mitigated continue to have radon levels above the EPA recommended guideline of 148 Bq/m<sup>3</sup> (4 pCi/l).<sup>2</sup> Diagnostics are therefore crucial for providing information relevant and necessary to the successful design and implementation of a radon mitigation system.

Subslab depressurization (SSD) has been widely adopted as a radon mitigation technique.<sup>1,3</sup> This method relies upon reducing the pressure under the slab to values below that of the basement (or living space in the case of slab-on-grade), at least at locations where soil gas flow into the basement could occur. In the pre-mitigation diagnostic phase, the degree of "connectivity"<sup>4</sup> under the slab as well as the permeability characteristics of the subslab medium must be determined before a suitable SSD system can be designed. Proper attention to these aspects will ensure that reasonable flows, and hence the desired degree of depressurization, will prevail at all points under the slab.

Parallel with the above aspect is the concern that presently mitigators tend to over-design SSD systems in order to err on the safe side. In so doing, more radon from the soil is removed and vented to the ambient air than would have occurred naturally.<sup>3</sup> There is an equal energy penalty associated with the over-design, since part of the conditioned basement or house air is also drawn, via cracks in the walls and in the slab, into the mitigation system. There is thus the need to downsize current overly robust SSD mitigation systems and decrease emission exhaust quantities of radon while simultaneously ensuring that indoor radon levels do not exceed the recommended value.

One aspect of our current research is the formulation and verification of a rapid diagnostic protocol for subslab and wall depressurization systems designed to control indoor radon levels.<sup>4</sup> The formulation of the diagnostics protocol consists of: (1) the specification of practical guidelines that would enhance the effectiveness of the engineering design of the radon mitigation system, and (2) the reliance on fundamental scientific studies that provide additional data

## Nomenclature

A	cross-sectional area of flow
a	parameter representative of the resistivity to flow of the porous bed
b	pressure drop exponent for turbulent flow in gravel beds
d	diameter
$d_v$	equivalent diameter of pebbles
g	acceleration due to gravity
h	thickness of the porous bed
k	permeability of porous bed
p	pressure
$p_a$	atmospheric pressure
q	total volume flow rate
$R^2$	coefficient of determination of regression
Re	Reynolds number
r	radial distance from center of the suction hole
$r_o$	outer radius of the laboratory apparatus
x	distance along flow
$\rho$	density
$\nu$	dynamic viscosity
$\phi$	porosity of porous bed

## Subscripts

a	air
b	porous bed
f	fluid
p	pipe
w	water

and insight needed to develop, test, and revise protocols. The present study specifically addresses the first of these, relying on current data and understanding and anticipating that additional data will become available to refine the approach taken here.

## Specification of the Problem

In terms of modeling the induced subslab pressure fields, the present housing stock construction can be broadly divided into three groups: (1) those with a gravel bed under the concrete slab, (2) those without, in which case soil is the medium under the slab, and (3) those houses which have both. In the case of (2), the soil permeabilities are much lower than case (1) and more careful design of the mitigation system is warranted. In New Jersey, houses less than about 30 years old typically have gravel beds about 0.05–0.1 m thick under the slab. However, other states seem to have very different construction practices: for example, housing construction in Florida uses slab on grade placed directly on compacted fine-grained soil which offers high resistance to air flow.

Figure 1a and 1b schematically depict the type of construction and the expected air flow paths one would typically expect in a house with either gravel or soil under the slab, when a single suction pressure is applied through the slab. (In case of a radon mitigation system using subslab pressurization, one could, to a good approximation, simply assume similar aerodynamic effects with the direction of air flows reversed.) Since the permeability of the gravel bed is usually very much higher than that of the soil below, one could assume, except for the irregular pattern around the footing which would occur over a relatively small length, that the subslab air flow is akin to radial flow between two impermeable circular disks with a spacing equal to the thickness of the gravel bed.<sup>5</sup> Note that this model equally accounts for the leakage of air from the basement when this leakage occurs from the perimeter cracks or through the basement wall.

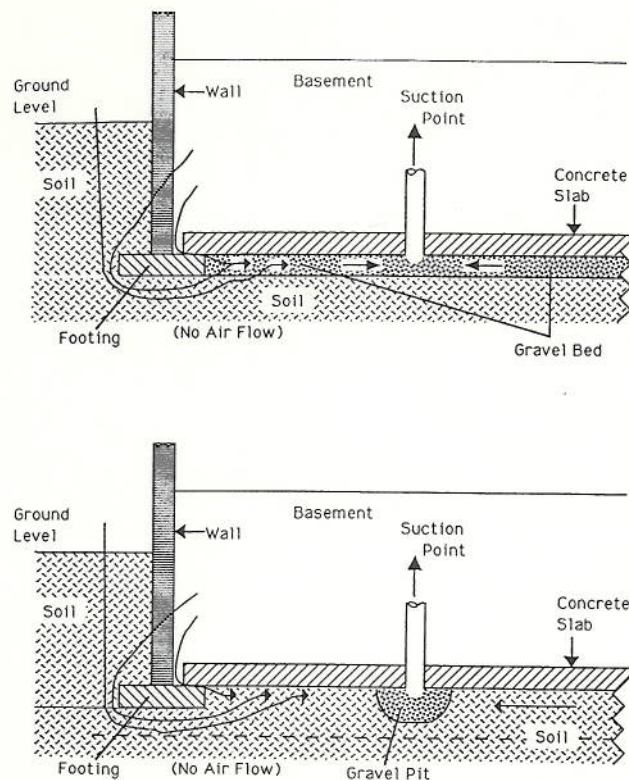


Figure 1. Schematic of a subslab mitigation system and the air flows in the basement of a house. Note that part of the air flowing through the subslab bed originates from the basement and the rest from the ambient air. Top—House with a gravel bed; Bottom—House with a soil bed.

In the case of a house without a gravel bed (Figure 1b), suction applied at a simple penetration through the slab (as in Figure 1a) is no longer practical since the area of depressurization is usually small. In order to enhance mitigation effectiveness, the current practice is to increase this area by either digging a gravel pit below the concrete slab or, more simply, by hollowing out a hemisphere of about 0.3–0.45 m radius underneath the suction hole. Even under such conditions, provided the soil underneath is free of major obstructions like concrete footings, duct work, piping, and large rocks, air flow can be approximated as occurring between two impermeable circular disks with a spacing equal to either the depth of the gravel pit or the radius of the hollow hemisphere.

## Preliminary Theoretical Considerations

The above discussion was intended primarily to suggest that flow underneath the slab be visualized as occurring in radial streamlines terminating at the central suction point. Note that such a representation would perhaps be too simplistic or even incorrect for a house with a part-basement (case 3 above). In the present study, we shall limit ourselves to understanding the flow and pressure drop characteristics through a *homogeneous bed* (of either gravel or soil) with *uniform boundary conditions*, the obvious one to start with being a circular configuration. The first question to be tackled relates to the nature of the flow, i.e., whether the flow is laminar or turbulent, and where, if at all, there is a transition from one regime to another. Current scientific thought is to distinguish four different flow regimes in porous media. Visualizing flow regimes as either laminar or turbulent as is done here is a simplification which we feel is justified in the present context. The Reynolds number gives an indication of the flow regime.<sup>6–7</sup> Though there is an inherent ambiguity in the definition of the quantity characterizing the length dimension, we shall

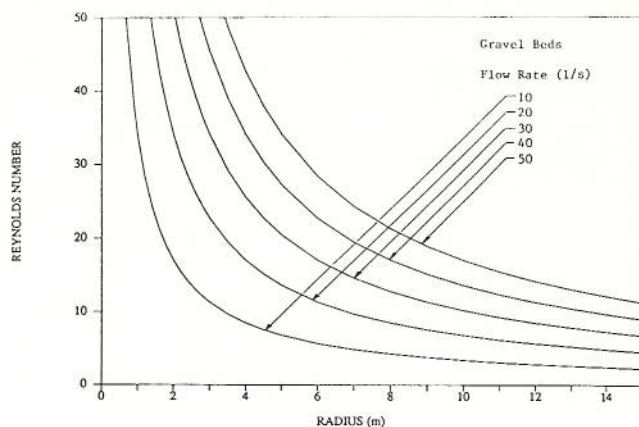


Figure 2. Expected Reynolds number for mitigation system air flow through subslab gravel beds. Radial cylindrical disk flow with impermeable boundaries is assumed with disk spacing = 0.1 m, diameter of gravel = 0.012 m, and porosity of bed = 0.4. Reynolds numbers above 10 indicate turbulent flow while below 1 correspond to laminar flow.

adhere to the following definition:

$$Re = \frac{q}{A} \cdot \frac{1}{v_a} \cdot \frac{d_v}{\phi} \quad (1)$$

where:

- $q$  = total volume flow rate
- $A$  = cross-sectional area of flow (in the case of radial flow through a circular bed of radius  $r$  and thickness  $h$ ,  $A = 2\pi rh$ )
- $v_a$  = kinematic viscosity of air
- $d_v$  = equivalent diameter of gravel or soil particles
- $\phi$  = void fraction or porosity of the gravel bed

Let us first look at flow through a gravel bed. Some typical values of the above parameters could be assumed:

$$h = 0.1 \text{ m}, d_v = 0.0125 \text{ m}, v_a \text{ (at } 15^\circ\text{C)} = 14.6 \times 10^{-6} \text{ m}^2/\text{s}, \text{ and } \phi = 0.4.$$

The values of  $q$  encountered in practice range from 10 to 50 l/s. Under these conditions the resulting Reynolds number for radial flow at different radii can be determined from Figure 2. A safe lower limit for turbulent flow is when  $Re > 10$ , and a safe upper limit for laminar flow is when  $Re < 1$ .<sup>6,7</sup> (The common held conception that turbulent flow occurs at Reynolds numbers of several thousands is valid only for flow inside tubes and ducts and not for flow in packed beds.) Since basements do not generally exceed 6 m in radius, we note from Figure 2 that subslab flow would tend to be largely turbulent when a gravel bed is present. This by itself is an important finding since explicit recognition of this aspect was not made in earlier studies.

On the other hand, in a house with soil as the subslab medium, the air flow through the soil is most likely to be laminar. Soil grain diameters range from 0.06 to 2 mm<sup>8</sup> and volume flow rates in corresponding mitigation systems are typically lower, about 0.8–6.0 l/s. Assuming some typical values of  $h = 0.1 \text{ m}$ ,  $\phi = 0.4$ , and  $q = 2.4 \text{ l/s}$ , the corresponding Reynolds numbers for air flow through sands of different grain diameters have been calculated from Equation 1 and are shown in Figure 3. We note that indeed the flow is likely to be laminar in most cases.

### Mathematical Model for Radial Flow

The core of any model is the formulation of the correlation structure between pressure drop and  $Re$  (or flow rate). For laminar flow, Darcy's Law holds and we have:<sup>6</sup>

$$\frac{1}{\rho_f \cdot g} \cdot \frac{dp}{dx} = a \cdot \frac{q}{A} \quad (2)$$

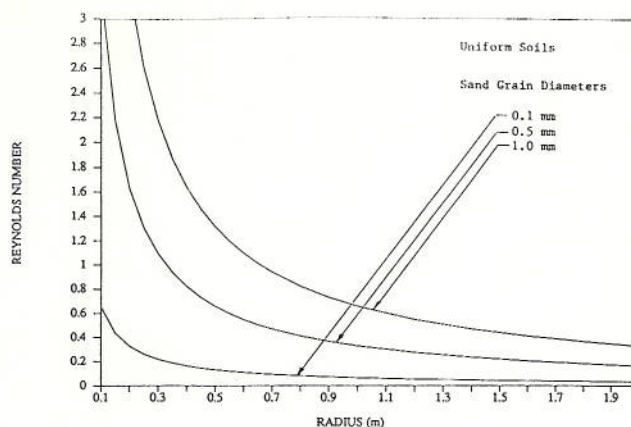


Figure 3. Expected Reynolds number for mitigation system air flows through subslab soil for houses without a subslab gravel bed. Radial cylindrical disk flow with impermeable boundaries is assumed with disk spacing = 0.1 m, flow rate = 2.4 l/s, and porosity of bed = 0.4. Reynolds numbers below 1 indicate laminar flow while between 1 and 10 correspond to the transition range.

where:

- $\rho_f$  = density of the flowing fluid
- $g$  = gravitational constant

For turbulent flows, a model such as the following is widely used:<sup>7</sup>

$$\frac{1}{\rho_f \cdot g} \cdot \frac{dp}{dx} = a \left( \frac{q}{A} \right)^b \quad (3)$$

The left side is the pressure drop per unit bed length, and can be loosely interpreted as the resistivity of the porous bed to the flow of the particular fluid. The permeability,  $k$ , of the porous bed is given by:

$$k = \frac{v_a}{g} \cdot \frac{1}{a} \quad (4)$$

We can derive a mathematical expression for the pressure field when suction is applied at the center of the circle (see Figure 4). We assume air flows radially through a circular homogeneous gravel bed. For the suction pressures encountered in this particular problem, air can be assumed to be an incompressible fluid. Thus assuming a simple model such as Equation 3 for the pressure drop yields:

$$\frac{d}{dr} \left( \frac{p(r)}{\rho_a \cdot g} \right) = a \cdot \left( \frac{q}{2\pi h} \right)^b \cdot \frac{1}{r^b} \quad (5)$$

where  $p(r)$  is the pressure of air at a radial distance  $r$  from the center and  $\rho_a$  is the density of air. Strictly, the distance should be taken from the outer edge of the suction pipe ( $r'$

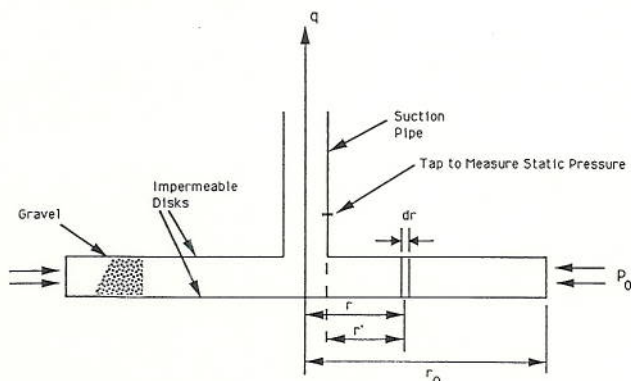


Figure 4. Schematic of a model to duplicate flow conditions occurring beneath the concrete slab of a residence when induced by a single suction point. The air flow is assumed to be radial flow through a homogeneous porous bed of circular boundary.

in Figure 4). The diameter of the suction pipe is typically small compared with the diameter of the disk, and one could neglect this difference without any error in the subsequent analysis.

Integrating Equation 5, and using the boundary conditions  $r = r_o$  and  $p = p_a$  at the edge of the disk, we have:

$$\frac{p(r) - p_a}{\rho_a \cdot g} = a \left( \frac{q}{2\pi h} \right)^b \cdot \frac{1}{1-b} \cdot (r^{1-b} - r_o^{1-b}) \quad (6)$$

Since the pressure drop is often measured in units of head of water, it is more convenient to modify the above equations to:

$$\frac{p(r) - p_a}{\rho_w \cdot g} = a \cdot \frac{\rho_a}{\rho_w} \cdot \left( \frac{q}{2\pi h} \right)^b \cdot \frac{1}{1-b} \cdot (r^{1-b} - r_o^{1-b}) \quad (7)$$

On the other hand, during laminar flow, Darcy's Law holds and the exponent  $b = 1$ . Under these circumstances, integrating Equation 5 with  $b = 1$  and inserting the appropriate boundary conditions yields:

$$\frac{p(r) - p_a}{\rho_w \cdot g} = a \cdot \frac{\rho_a}{\rho_w} \cdot \frac{q}{2\pi h} \cdot \ln \left( \frac{r}{r_o} \right) \quad (8)$$

It is easy to modify these equations to apply to outward radial flow as one would encounter in houses where the subslab pressurization technique is used. The boundary conditions are still the same but now the pressure at the throat of the suction pipe is higher than ambient pressure and the quantity  $[p(r) - p_a]$  is positive and represents the pressure above the ambient pressure.

If parameters  $a$  and  $b$  are constant for a given bed material and can be determined by actual experiments in the field, they will serve as indices for mitigation system design.

## Laboratory Apparatus

One needs to evaluate the soundness of the mathematical derivation presented above and also to determine the numerical values of the empirical coefficients of Equation 3. To this end, a laboratory model consisting of a 2.4 m diameter circular section that is 0.15 m deep was constructed. The top and bottom impermeable disks were made from 0.02 m thick plywood, and a wire mesh at the outer periphery of the disks was used to contain the gravel between the two disks. The apparatus allowed experiments to be conducted with a maximum disk spacing (or depth of gravel bed) of 0.095 m. An open-cell foam sheet 0.025 m thick was glued to the underside of the top plywood disk. During the experiments, heavy weights were placed on top of the plywood disk, thus effectively eliminating gaps that may exist between the disk and the gravel top which could cause short-circuiting of the air flow.\* This guarantees that air flow occurs through the bed and not over it.

The total volume of the packed bed is approximately 0.43 m<sup>3</sup> which, for river-run gravel, translates into a net weight of about 700 kg (1530 lb).

A 0.038 m diameter hole was drilled at the center of the top disk to serve as the suction hole. Nine holes were drilled on three separate rays of the top disk and a PVC pipe of 0.012 m inner diameter with chamfered ends was press-fit into these holes so that they terminated at the bottom side of the disk and did not extend into the gravel. Pressure measurements at these nine holes would then yield an accurate picture of the pressure field over the entire bed.

Equipment needed for the experiments included:

1. An industrial vacuum cleaner capable of sucking  $45 \times 10^{-3}$  m<sup>3</sup>/s (95 cfm) of air through a 0.05 m (2 in.)

diameter orifice under 1.9 m (75 in.) of water static vacuum pressure.

2. A speed control and an air by-pass adapter (which is simply a perforated length of plastic pipe). Both of these are needed in order to vary the air flow rate through the porous bed.
3. A 3 mm stainless steel pitot tube (Dwyer No. 166-6) to measure velocities from 0.05 to 15 m/s (10 to 3000 ft/min). Tables for different pipe diameters (as described in Reference 4) enabled the corresponding volume flow rate to be deduced.
4. An electric digital micromanometer (EDM) (Neotronics Model EDM-1) which can measure pressures with a resolution of  $0.025 \times 10^{-3}$  m ( $10^{-3}$  in.) of water or 0.25 Pa, and having a maximum range of up to 0.5 m (20 in.) of water. This is also described in Reference 4.

Other apparatus included two mounting devices: (1) a 0.038 m (1.5 in.) outer diameter brass pipe to connect the suction hole to the vacuum hose with arrangements to attach the pitot tube [called the Flow Pressure Tube (FPT)] and the EDM; and (2) a 0.019 m (0.75 in.) stainless steel pipe to mount the EDM in order to measure the pressure at each of the nine different taps. These devices have already been described in detail in a previous report.<sup>4</sup>

We chose a predetermined total air flow rate and gradually controlled the speed of the suction fan in order to achieve this flow. The pressure measurements (representative of the corresponding static pressure inside the porous bed) at each of the nine taps were taken with all other taps closed. This completed a series of readings pertaining to one run. In subsequent runs, the total air flow rate was set to another predetermined value and the readings were repeated.

## Experimental Results and Analysis of Radial Flow

Table I summarizes the different experiments performed using the laboratory apparatus. For example, Experiment A involved river-run gravel of nominal diameters of 0.012 and 0.019 m which we shall refer to as small and large gravel, respectively. Experiments A1 and A2 differ only in the spacing between the plywood disks; i.e., the thickness of the bed was altered. Experiment A1 involved three separate runs each with a different total volume flow rate, the specific values of which are also given in Table 1. The flow regime (as specified by the corresponding calculated Reynolds number) was found to be turbulent throughout the radial disk.

The specific values of the mean gravel diameter and the porosity of the bed are required for computing the Reynolds number [given by Equation 1]. Least square regression for both the constant 'a' and exponent 'b' was performed on the observed experimental pressure drop data using Equation

**Table I.** Summary of the different experiments using river-run gravel performed with the laboratory apparatus under turbulent flow conditions.

Experiment	Gravel size (nominal diameter) (m)	Disk spacing (m)	No. of runs	Total flow rate (l/s)
A1	0.012	0.075	3	20.5 30.1 37.3
A2	0.012	0.10	2	22.1 31.4
A3	0.019	0.10	4	11.2 15.2 17.6 20.8

\*Experiments performed with the same gravel type for different bed thicknesses yielded identical permeability values. This suggested that the open-cell foam was effective in eliminating air gaps between the disk and the gravel top.

**Table II.** Summary of various laboratory experiments performed and the physical parameters deduced in the framework of the present study using river-run gravel.

Experiment	Diameter of particles		Measured porosity	R <sup>2</sup>	Pressure drop exponent	Permeability of bed(m <sup>2</sup> )
	nominal (m)	measured (m)				
A1 + A2	0.012	0.011	0.374	0.99	1.60	$9.4 \times 10^{-9}$
A3	0.019	0.022	0.424	0.99	1.40	$34 \times 10^{-9}$

7. We note that R<sup>2</sup> values are very high (Table 2) and one cannot realistically expect better fits (given the measurements errors in our readings, we may in fact be overfitting in the sense that we are trying to assign physical meaning to random errors). This is illustrated by Figure 5 where we note that the fit between model predictions and observed pressure drop is very good.

The study referred to earlier<sup>5</sup> found values of the exponent *b* to be 1.56 for the cylindrical disk model. This is generally borne out in the present study where we find *b* = 1.6 for the small river-run gravel and *b* = 1.4 for the large gravel.

The values of permeability of the porous bed calculated following Equation 4 are included in Table II and show a threefold difference between small and large gravel sizes. The numerical values do seem to correspond to those cited in the radon literature.<sup>8,9</sup>

### Field Verification

The irregular boundary conditions and the non-homogeneity in subslab beds that arise in practice are however not easily tractable with a simple expression such as Equations 7 and 8, and resorting to a numerical computer code may be the only rigorous way to proceed in order to predict pressure fields under actual situations.<sup>10,11</sup> We shall show in this section that our simplified approach nevertheless has practical relevance because it could be used to determine which areas under the slab have poorer connectivity.

The house under investigation (H21) has a partial basement with a gravel bed under the basement slab. As shown in Figure 6, the basement (though rectangular) is close to being square (6.45 × 7.60 m). It has two sides exposed to the ambient air above grade, while the other two sides are adjacent to slab-on-grade construction. One suction hole of 0.1 m diameter was drilled at roughly the center of the basement slab to which a temporary mitigation system was installed. Though 19 holes were drilled through the slab (Figure 6), two of them (holes 11 and 12) were found to be blocked beneath the slab. Consequently, data from only 17 holes have been used in this study. This blockage was later

found to be due to the presence of an oversized footing for a support column.

Three sets of runs were carried out which, depending on the air flow rate through the single suction pipe, are termed:

1. 28 l/s—High flow,
2. 23.4 l/s—Medium flow
3. 18.1 l/s—Low flow.

Note that our analytical expression for the pressure field under turbulent flow given by Equation 7 is strictly valid for a circular disk with boundary conditions at  $r = r_0$  and  $p = p_a$ . We approximate the rectangular basement by a circle of 3.5 m mean radius. We need to also include the extra path length of ambient air flowing down the outer basement wall, going under the footing, and then flowing through the subslab gravel into the suction hole. We estimate this to be about 2 m. An approximate way of dealing with this aspect is to overlook the fact that the soil around the house is generally less permeable than the gravel, and assume similar flow characteristics for both. Consequently, we find that  $r_0 = 5.5$  m. The thickness of the subslab gravel bed, *h*, has been found to be about 0.05 m.

The gravel under the slab, though river-run, was found to be highly heterogeneous in size and shape. In general, its average size was slightly less than 0.012 m. However, we decided to use the properties of the 0.012 m gravel determined experimentally in the laboratory (see Table 2).

Figure 7a and 7b show the observed and calculated pressure drops for two different total air flow rates. Readings from holes 13 and 14 are lower than predicted and we suspect poorer connectivity to these holes; i.e., some sort of blockage in this general area. We note that the agreement between model and observation (Figure 7) is indeed strik-

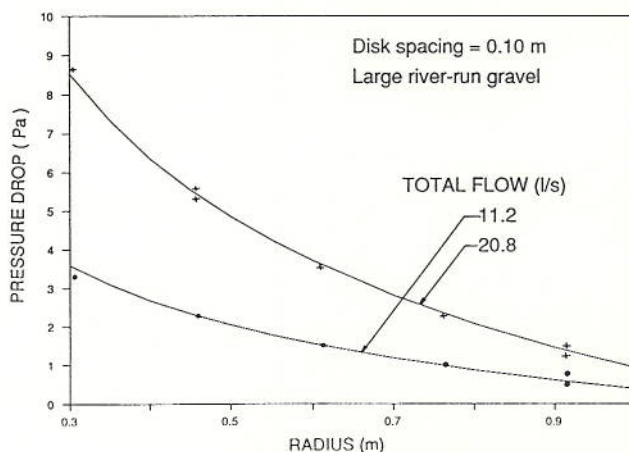


**Figure 5.** Comparison of observed and regressed pressure drops using the laboratory apparatus. Exps. A3 with *b* = 1.4.

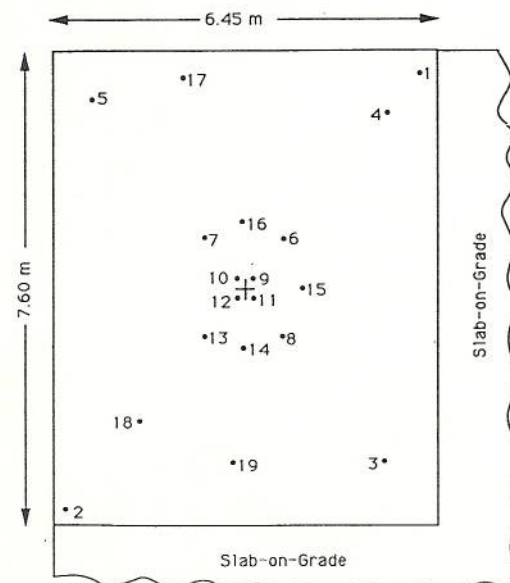


**Figure 6.** Plan of the basement slab of House H21 showing the relative positions of the various subslab penetrations. The suction hole of the mitigation system is marked as +.

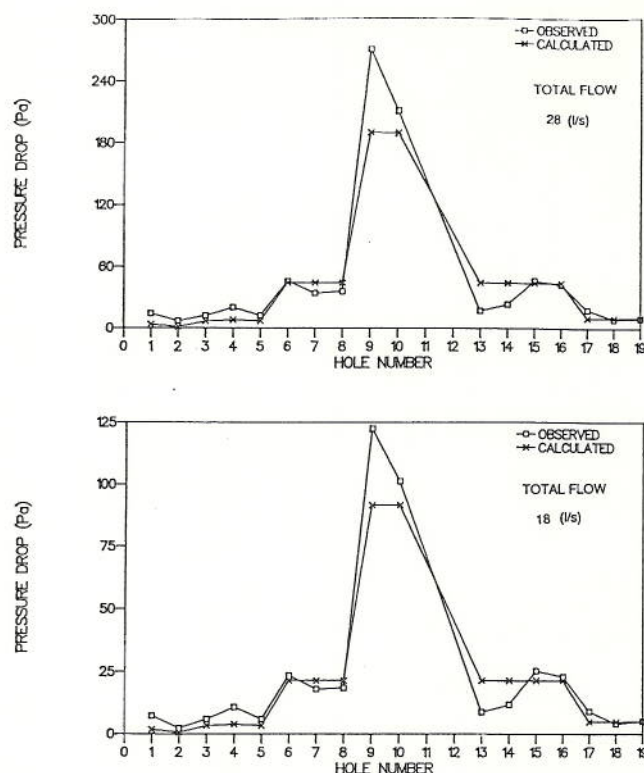


Figure 7. Comparison of observed and estimated pressure drops in House H21 using coefficients of 0.012 m gravel. Data of blocked holes 11 and 12 are not included.

ing, given the simplification in our model and also the various assumptions outlined above.

Figure 7 indicates which areas under the slab are non-uniform. A better way of illustrating how well the model fares against actual observations is shown in Figure 8. The solid line represents the model predictions while observa-

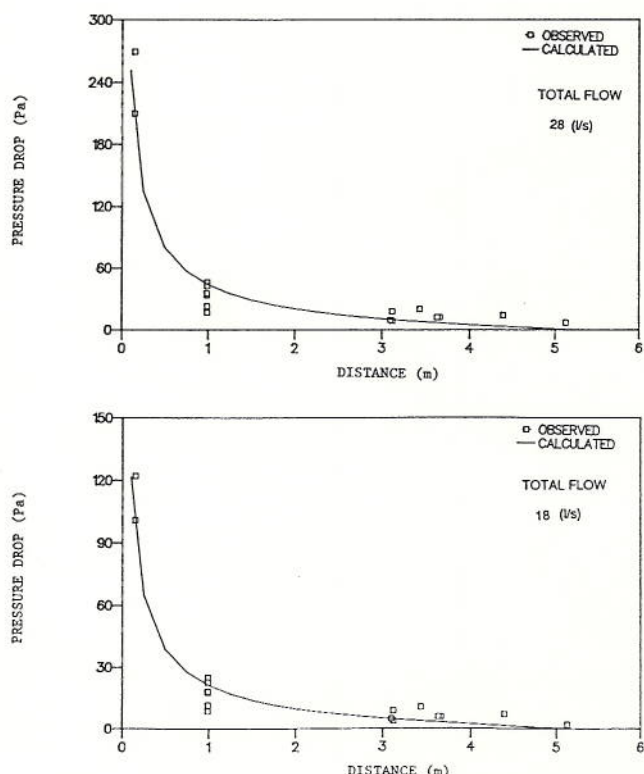


Figure 8. Comparison of observed and computed pressure drops using coefficients of 0.012 m gravel. Data of blocked hole 12 are not included.

Table III. Results of regressing experimental data using Equation 7.

Trial run	b	k (m <sup>2</sup> )	SEM (%)	R <sup>2</sup>	Remarks
1	1.6	$9.3 \times 10^{-9}$	6.7	0.80	With all data points
	1.7	$7.5 \times 10^{-9}$		0.80	
2	1.6	$7.1 \times 10^{-9}$	3	0.96	With data of holes 11 and 12 removed
	1.7	$5.8 \times 10^{-9}$		0.97	
3	1.6	$10.0 \times 10^{-9}$	5	0.88	With data of holes 9, 10, 11, and 12 removed
	1.7	$7.3 \times 10^{-9}$		0.87	

tions are shown by discrete points. We note again the satisfactory predictive ability of this modeling approach and also the fact that certain holes have pressure drop values higher than those predicted by the model.

An alternate approach to the one adopted here and described above would be not to assume specific gravel bed coefficients but to determine these from regression. This entails using Equation 7 along with the data set of actual observations and determining the parameters  $a$  (and the permeability  $k$ ) and  $b$  by regression. Since  $b$  is not a parameter that varies greatly, we have chosen two different values of  $b$  (1.6 and 1.7) to see what difference this leads to in terms of the coefficient of determination ( $R^2$ ) of the regression and in the values of  $k$ .

Regression results are summarized in Table III. We have performed three trial runs. Trial 1 uses all data points. In Trial 2, pressure drop observations from holes 11 and 12 (holes that are blocked) have been removed. We note that the  $R^2$  improves dramatically, from 0.80 to 0.96. For Trial 3, holes 9 and 10 have also been removed in order not to bias the regression since these holes have high pressure drop values. We note that the  $R^2$  of Trial 3 is 0.88, an improvement over that of Trial 1.

Other than the very high  $R^2$  values found, the most striking feature is that regression yields a value of  $k$  which is practically identical to that of the 0.012 m gravel determined experimentally in our laboratory apparatus. This suggests that even a visual inspection of the porous material under the slab could possibly be an indicator good enough for a mitigator to select a standard bed material from a table before using the physical properties of the material to get a sound estimate of what the suction pressure ought to be in order to generate a certain pressure field under the slab. The need to categorize commonly found subslab material, deduce their aerodynamic pressure drop coefficients in laboratory experiments, and then tabulate these in handbooks seems to be worth investigating.

## Summary and Future Work

We build upon the suggestion of a prior study<sup>5</sup> that flow under the slab of a house during mitigation using the subslab depressurization (and the pressurization) technique be likened to radial flow between two impermeable disks. A mathematical treatment to analytically predict the pressure field in homogeneous circular porous beds when subjected to a single central suction hole is presented. A laboratory apparatus constructed so that it can specifically duplicate conditions which occur in practice under slabs of real houses being mitigated for radon using the depressurization (or the pressurization) technique is then described. The experimental procedure followed in order to measure the pressure field of turbulent air flow is outlined from which the regression coefficients of the pressure drop versus flow correlation can be determined. Preliminary field verification results of our modeling approach in a house with gravel under the basement slab are presented and discussed. Though our simple model yielded very good

predictions of the pressure field extension in a single house with a subslab gravel bed, validation in more houses and in houses with soil as the subslab medium is required before this modeling approach can be accepted with confidence as a diagnostic tool. A striking conclusion of our study is that even a visual inspection of the porous material under the slab may possibly be an indicator good enough for a sound engineering design, if used in parallel with our modeling approach and given a table containing the aerodynamic pressure drop coefficients of commonly found subslab material.

Logical extension of this approach would be to adapt this modeling approach to the design of SSD systems themselves. This would involve application of this methodology to houses with (1) homogeneous beds but with irregular boundaries, and (2) non-homogeneous porous beds. One approach is to develop a simplified computer program using numerical methods (either finite element or finite difference could be used) to solve the basic set of aerodynamic and mass conservation equations.<sup>10,11</sup> Pressure fields under the slab for practically any configuration could be thereby predicted. An optimization algorithm could then be attached to the above program in order to obtain the optimal layout and the number of mitigation suction points for the particular subslab conditions such that certain well-defined and physically relevant constraints are satisfied.

Our present line of thinking is that, though the above approach offers great flexibility, it is not easy to use by non-experts. Developing engineering guidelines for practitioners based on such a code demands a certain amount of effort and practical acumen. It would be wiser to define a few "standard" cases of basement shape, subslab conditions, and mitigation pipe locations; try to develop simplified closed-form solutions of these cases; and then see how well these solutions fare with respect to actual measurements taken in the field. If such an approach does give satisfactory engineering accuracy, its subsequent use as an engineering design tool, well within the expertise of the professional community, seems promising.

## Acknowledgments

The assistance of R. Gafgen during the experimental phase of this study is acknowledged as also is that of D. Hull for his insight into certain statistical aspects. Fruitful discussions and insights into fundamental hydrological concepts by Prof. G. F. Pinder and J. Guarnaccia were invaluable during the initial stages of this study. This research is part of Cooperative Agreement CR 814673 funded by the U.S. Environmental Protection Agency. Critical comments and encouragement by D. Sanchez, R. Mosley and others of U.S. EPA, AEERL, RMB are acknowl-

edged. One of us (RGS) acknowledges the partial support of the Hewlett Foundation during his stay at Princeton University. Insightful comments by the reviewers of this paper are also acknowledged.

## References

1. Harrie, D. T.; Hubbard, L. M. *Proceedings of the Radon Diagnostics Workshop*, April 13-14, 1987, EPA-600/9-89-057 (NTIS PB89-207898), June 1989.
2. Wang, J.; Cahill, M. "Radon Reduction Efforts in New Jersey," paper presented at the Annual Meeting of the National Health Physics Society, Boston, MA, July 4-8, 1988.
3. Sanchez, D. C. "Technical Issues Related to Emission Releases from Subslab Radon Mitigation Systems," presented at ASCE National Conference on Environmental Engineering, Austin, TX, July 9-12, 1989.
4. Gadsby, K. J.; Hubbard, L. M.; Harrie, D. T.; Sanchez, D. C. "Rapid Diagnostics: Subslab and Wall Depressurization Systems for Control of Indoor Radon," in *Proceedings: The 1988 Symposium on Radon and Radon Reduction Technology*, Volume 2, EPA-600/9-89-006b (NTIS PB89-167498), March 1989.
5. Matthews, T. G.; Wilson, D. L.; TerKonda, P. K.; Saultz, R. J.; Goolsby, G.; Burns, S. E.; Haas, J. W. "Radon Diagnostics: Subslab Communication and Permeability Measurements," in *Proceedings: The 1988 Symposium on Radon and Radon Reduction Technology*, Volume 1, EPA-600/9-89-006a (NTIS PB89-167480), March 1989.
6. Muskat, M. *The Flow of Homogeneous Fluids through Porous Media*, McGraw-Hill, New York, 1937.
7. Scheidegger, A. E. *The Physics of Flow Through Porous Media*, Univ. of Toronto Press, 3rd Edition, 1974.
8. Nazaroff, W. W.; Moed, B. A.; Sextro, R. G. "Soil as a Source of Indoor Radon Generation, Mitigation and Entry," in *Radon and Its Decay Products in Indoor Air*, W. W. Nazaroff and A. V. Nero, Eds., John Wiley and Sons, NY, 1988, chap 2.
9. *Radon and Its Decay Products*, Hopke, P. K., Ed., American Chemical Society, 1987.
10. de O. Loureiro, C. "Simulation of the Steady-State Transport of Radon from Soil into Houses with Basement under Constant Negative Pressure," report LBL-24378, Lawrence Berkeley Laboratory, Berkeley, CA, 1987.
11. Barbar, J. M.; Hintenlang, D. E. "Computer Modeling of Subslab Ventilation Systems in Florida," paper presented at the 34th Annual Meeting of Health Physics, Abstract No. TAM-E8, Albuquerque, NM, 1989.

At the time of writing, T. A. Reddy, K. J. Gadsby, H. E. Black, III, and D. T. Harrie were with Princeton University, School of Engineering/Applied Science, Center for Energy and Environmental Studies, Princeton, NJ 08544. T.A. Reddy is currently with Texas A & M University, Department of Mechanical Engineering, College Station, TX 77843-3123. R.G. Sextro is with the Indoor Environment Program, Lawrence Berkeley Laboratory, Berkeley, CA 94720. This manuscript was submitted for peer review on March 20, 1990. The revised manuscript was received on May 24, 1991.